Research Article Adv. Mat. Lett. 2013, **4**(6), 464-475 ADVANCED MATERIALS *Letters*

www.amlett.com, www.amlett.org, DOI: 10.5185/amlett.2012.ib.115
"Nanostructuring by electrons, photons and ions" Special Issue Published online by the VBRI press in 2013

Sensor grade nanostructured thin films of multicomponent semiconducting oxide materials by pulsed laser deposition

K. I. Gnanasekar, E. Prabhu, V. Jayaraman, T. Gnanasekaran*

Liquid Metals and Structural Chemistry Division, Indira Gandhi Centre for Atomic Research, Kalpakkam – 603 102, India

*Corresponding author. Fax: (+91) 44 274800659; E-mail: gnani@igcar.gov.in

Received: 16 March 2012, Revised: 22 July 2012 and Accepted: 26 July 2012

ABSTRACT

High quality sensor grade nanostructured thin films of multicomponent semiconducting oxide sensors with superior sensitivity for monitoring trace levels of pollutant gases like NO_x, NH_3, H_2 etc., in the ambient have been deposited by pulsed laser deposition technique. In-situ growth carried out at relatively lower temperatures yield granular films composed of nanocrystals of the desired crystallographic phase which otherwise would require high temperatures to stabilize. At some specific deposition conditions, growth of thin films containing uniform sized nano-grains with optimum inter-granular connectivity can be readily achieved. Here, we present the superior sensing properties of the sensor grade films of selected materials and bring out the unique characteristics of pulsed laser deposition technique for exploratory research in nano-structured thin films of materials not amenable to conventional synthetic routes. Copyright © 2013 VBRI press.

Keywords: Pulsed laser deposition; nanostructured thin films; chemical sensors; pollutant gases.

V. Jayaraman is from 32nd batch of BARC Training School and started his research career in IGCAR, Kalpakkam from 1989. Research areas of his interest are solid electrolytes, chemical sensors for ambient monitoring and soft chemical synthesis of multicomponent oxides.

T. Gnanasekaran received his Masters degree in Chemistry from University of Madras in 1973 and Ph.D. in 1987. He is from 17th batch of BARC training school. He has been a scientist with IGCAR, Kalpakkam since 1974. His main research interests are chemical sensors, high temperature thermochemistry, alkali and heavy metals chemistry.

Introduction

Thin films have become the centre of investigation in materials research and were exploited for a variety of technological applications [**1-3**]. Some applications require high quality single crystal epitaxial thin films free of defects. Others require predominantly textured growth with a specific orientation exploiting the anisotropic properties of the material. Still certain other applications prefer thin films composed of uniform nanocrystals with grains of specified size range and uniform distribution [**4**]. Depending on the nature of the application, thin films with the desired features are prepared.

Materials exhibiting interesting properties are complex oxides, nitrides, carbides, inter-metallic alloys etc., and therefore, a more general technique is necessary to grow nanostructured thin films of any material. The drive for the basic research on nanostructured thin films primarily comes from the fascinating science exhibited by the conventional/new materials when constrained by size. Although a variety of physico-chemical methods have been explored to synthesize materials in specific grain size, not all the materials can be synthesized in the desired form as many of them are not amenable to low temperature processing. Although, chemical techniques like CVD, MOCVD have been shown to be useful for synthesis of high quality nanostructured thin films directly, only limited materials could be successfully grown as thin films [**5**]. These techniques, however, were very useful for large scale synthesis of thin films of those limited materials. Hence, a simple, elegant thin film technique which offers the flexibility in preparation of thin films in the prescribed configuration composed of uniform grains in the preferred size range would be highly appropriate for exploratory investigations. In addition to that, the chosen thin film growth technique should help in testing the predicted concepts in structures such as multilayers, superlattices or nanocrystalline thin films quickly and reliably without spending much time on optimization of growth parameters.

Recently, environmental protection has become one of the major inter-disciplinary subjects in the context of increasing number of chemical, petrochemical and coal based industries. The effluent gases discharged from these industries need to be continuously monitored in order to ensure that the pollutant gases are kept within the prescribed limit. Therefore, there is an urgency to develop compact, accurate and reliable sensing devices for on-line monitoring of trace levels of various pollutant gases in order to ensure environmental safety and protection. Driven by the large specific surface are to volume ratio, nanostructured thin films offer the potential to develop highly sensing devices. Here, we demonstrate the unique feature of pulsed laser deposition technique for direct growth of highly sensitive nanostructured thin films of complex multicomponent oxide materials including those which not amenable by other synthetic routes. The general requirement of the gas sensing thin films are addressed with illustrations from the author's laboratory and the related issues are highlighted.

General characteristics of sensor grade thin films for use as chemical sensors for pollutant gases

Semiconducting oxides exhibit a change in their conductivity in the presence of trace levels of pollutant gases and this property is exploited for making devices for online monitoring of specific pollutant gas [**6-9**]. The mechanism of sensing involves a chemical reaction of the surface chemisorbed oxygen with the target gas at suitable operating temperature. His sensitivity is necessary for reliable detection gases at the concentration of 1 to 50 ppm. To achieve this, the probability of the chemical interaction of the gaseous species with the surface of the semiconductor materials has to be maximized which in turn depends on the relative change in conductivity.

As chemical sensing is a surface phenomenon, the probability of the chemical interaction between the gas at trace level concentration and the semiconductor surface can be maximized in configurations offering high specific surface area such as porous bodies, thick films composed of nanocrystalline grains and nanostructured thin films. This chemical reaction is a redox reaction taking place on the surface resulting in loss or gain of electrons to the surface. Depending on the surface coverage of the adsorbed oxygen and the concentration of the analyte gas, the number of electrons released to the solid determines the change in conductivity of the solid and hence the sensitivity. In order to maximize the overall change in conductivity for measuring sensitivity, the surface conductivity has to be maximized which is accomplished by increasing the surface area offered by the porous structures. Alternatively, structures composed of grains with decreasing size also offer high specific surface area. Therefore, both the configurations offer the scope to alter the surface conductivity for this specific application. The schematic diagram of a grain of a semiconductor oxide along with the formation of depletion layer due to the abrupt termination of periodicity at the surface is shown **Fig. 1** [**8**]. The unsaturated dangling bonds of the surface serve as ideal sites for chemisorption of highly electron withdrawing gaseous oxygen species, which increases the width of the depletion layer thereby trapping the mobile charge carriers of the grain on the surface. The depletion layer is a highly resistive layer, whose width is represented by Debye length (L_D) given by the expression

$$L_D = \left[\frac{kT\varepsilon}{q^2 n} \right]^{1/2}$$

here k, T, q, ε and n are the Boltzman constant, absolute temperature, electron charge, dielectric constant and charge carrier concentration respectively [**6,10**]. In this expression, L_D depends on the charge carrier density and dielectric constant of the material. As L_D is characteristic of a given material, if the grain size is reduced gradually, one eventually gets down to situation where the grain size of about $2 \times L_D$ wherein the entire grain is exhausted of all electrons and the conduction carriers are localized on the surface.

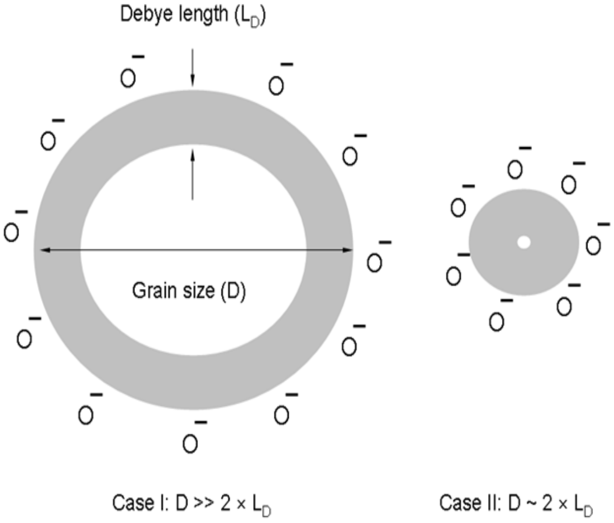

Fig. 1. Schematic diagram of a grain of a semiconductor oxide showing the carrier rich grain and the carrier depleted layer

In other words, the surface conductivity is maximized and any change in the electrical conductivity is purely due to changes in surface reactions. Another crucial parameter is how well these grains are interconnected. Although a grain with size $2 \times L_D$ gives the maximum signal, the signals arising from all grains that participate in chemical sensing have to be integrated which in turn depends on the inter-granular coupling. The schematic diagram of the alignment of grains is shown in **Fig. 2**. Therefore, alignment of grains has been a crucial factor to be optimized during in-situ growth and the well aligned granular film is shown in **Fig. 2**(a). Poorly aligned grains will lead to weak coupling despite the size of is $2 \times L_D$ and the sensor signal (sensitivity) which depends on the change in conductivity will be low. Depending on the size of the grain, three different mechanisms which control electrical conductivity viz. grain controlled, grain boundary controlled and neck controlled have been proposed [**4,10,11**]. These mechanisms are explained using a schematic diagram shown in **Fig. 3**. If the grain size is larger than $2 \times L_D$, then the mechanism which controls the electrical conduction is primarily the width of the depletion layer or grain boundary as shown in **Fig. 3**(a). If the average grain size is less than $2 \times L_D$, then all the grains are completely depleted and the mechanism which controls the conductivity in thin films is grain as shown in **Fig. 3**(b). When the grain size is equal to $2 \times L_D$, then a neck controlled conduction mechanism operates as shown in **Fig. 3**(c). It is this configuration which gives the highest sensitivity and becomes our object to realize in the nanostructured thin films [**10, 11**].

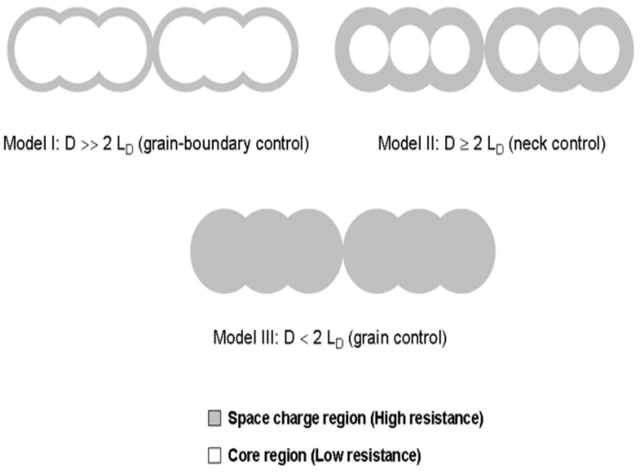

Fig. 2. Schematic diagram of the alignment of grains in thin films: (a) Well aligned grains with good inter-granular coupling (b) Poorly aligned grains and weak inter-granular coupling.

Porous bodies or thick films require nanocrystalline precursors of the compound which involves the identification of suitable synthetic route and the optimization of synthetic parameters for producing nanocrystals in desired size range and distribution. The next objective is to transfer the nanocrystalline powders on to thick or thin films using appropriate coating technology. This step involves a heating procedure for the adherence of the film on to the substrate during which, there is a possibility of grain growth beyond the desired nanocrystalline range [**11**]. The surface area to volume ratio of the porous bodies is relatively low, which makes the regeneration of the sensors taking longer time after the exposure.

Alternatively, nanostructured thin film configuration offers high specific area to volume ratio and therefore, the thin film growth technique which directly gives nanostructured films in a single step thereby avoiding lengthy optimization procedures would be the ideal choice. As the chemical sensing materials are mostly multicomponent semiconducting oxides with components having different vapour pressures, the first step is to transfer the target stoichiometry on to the thin films to avoid any compositional change. Secondly, a low temperature processing is necessary to realize the stabilization of the required phase in nanocrystalline form.

A brief survey of thin film growth techniques

The ideal conditions required for the growth of high quality nanostructured thin films can be summarized below [**12**]:

1. The provision for atoms of the multicomponent materials to arrive at the substrate at precise ratio
2. The ability to operate at high partial pressure of reactive gases in order to adjust the non-stoichiometry of oxygen/nitrogen or other gases besides forcing the volatile components to remain in thin film.
3. An extrinsic heating facility or an intrinsic mechanism by which each atom/ion is given a few tens of electron volts kinetic energy so that the in-situ growth of films is accomplished at substantially lower growth temperatures with the necessary adhesion strength.

Although, the conditions mentioned may appear simple, they are not met by any single deposition method. To begin with, thermal evaporation is the simplest and the easiest of all the techniques wherein the material to be deposited as thin film is evaporated using a resistive heating. This technique is successful for depositing one component or two component systems whose vapour pressures are comparable. However, for systems having more than two components this technique fails to satisfy even the first step mentioned above as the difference in vapour pressures of the components lead to incongruent evaporation giving rise to non-stoichiometric films. On the other hand, the sophisticated e-beam evaporation wherein a high energy electron beam is used to evaporate the components provides better stoichiometry as compared to the resistive evaporation. Being an equilibrium process, it is successful to some extent, yet the fundamental problem related to the stoichiometry of the volatile species of the multicomponent oxides persists. This technique also fails to satisfy the first step. There is another method known as flash evaporation which uses the concept of a flash heating to vaporize the components simultaneously in order to avoid the fractional evaporation, looked promising but does not produce the desired results. All these techniques require high vacuum better than 10^{-6} mbar during film growth which generally yields amorphous films. In-situ heating also does not produce the crystalline films in many cases, as the oxide films require an oxygen partial pressure ($> 10^{-2}$ mbar) during growth which is not possible by these techniques. Hence, these techniques need a post annealing at elevated temperatures for the formation of required crystallographic phase which is not recommended as this procedure leads to grain growth.

The most useful method for deposition of high quality thin films is the sputtering, widely employed in semiconductor industry for depositing multicomponent materials. Here, the mechanism does not involve thermal energy as used in evaporation and therefore the problems faced with the evaporation techniques are eliminated. In sputtering, the heavy gaseous ions usually argon are accelerated under the influence of high electric field. In magnetron sputtering, an additional magnetic field is introduced to increase the efficiency of the process. The momentum acquired by these ions under the influence of high electric field is transferred to the surface atoms of the target when they strike the target causing the surface atoms to sputter away. Thin films can be grown at relatively higher oxygen partial pressures of background gas allowing the in-situ formation of the crystallographic phase. The use of higher partial pressure of gases introduced during in-situ growth of thin films not only suppresses the evaporation of volatile species deposited on the heated substrate, but also keeps the oxygen nonstoichiometry of the compound comparable to the original value. Although this technique has been very useful in preparation of high quality thin films, it has certain limitation for depositing oxide materials. The oxygen introduced along with the sputter gas, gets negatively charged under the influence of the same electric field used to ionize and accelerate the argon atoms, and these oxygen ions sputter anode wherein the thin film growth is taking place, thus severely degrading the quality of the films. This enforces introduction of additional sophistication which eventually complicates the optimization of parameters for producing the high quality thin films by this technique.

Therefore, a better alternative without aforementioned constrains is desirable for depositing oxide materials. Tracking back to the fundamentals of the thin film growth by evaporation which is an equilibrium phenomenon, the fractional evaporation of components of the multicomponent oxide having lower vapour pressures are not suppressed, which gives rise to continuously varying plume composition at a given temperature. Although, the flash evaporation attempts to accelerate the evaporation kinetics of all the components without giving sufficient time for fractional evaporation to set-in, still this technique could not succeed as it does not completely eliminate the problem. Creative minds have reasoned that if the equilibrium conditions that prevail during evaporation are eliminated, then the problems associated with the fractional vaporization can be minimized and one can realize stoichiometric films. The use of high energy radiation in a pulsed mode with short pulse duration such as lasers have become a natural choice and is expected to provide the extreme non-equilibrium conditions with congruent evaporation.

The first attempt of laser for growing thin films was reported in 1965 which uses the then available ruby laser [**13**]. The films grown by this laser were inferior in quality when compared those films grown by conventional sputtering method. The choice of laser, wavelength and pulse energies were very limited and therefore, thin film growth by laser was not pursued with intensity. However, after the advent of Q switching technology offering short pulse width with high pulse energy, thin film growth again picked up and thin films of many materials were deposited with some success. However, the real breakthrough came when Venky and coworkers demonstrated the successful deposition of high quality thin films of $YBa_2Cu_3O_7$, a complicated multicomponent oxide superconductor not amenable to the conventional techniques [**14**]. Since then a variety of complex materials were grown by pulsed laser technique using excimer laser ablation. With the availability of variety excimer lasers operating at different UV wavelengths, thin film growth by pulse laser deposition has proved to be the best technique for growing thin films of complicated materials with ease.

Pulsed laser deposition of thin film growth

The two main components of the laser deposition are vaporization and ablation [**15**]. When the laser pulse duration is microseconds or longer and the irradiance is less then approximately 1 Mega Watt per square centimeter, vaporization is likely a dominant process influencing material removal from a target. Phonon relaxation rates are on the order of 0. 1 picosecond and absorbed optical energy is rapidly converted into heat. Heat dissipation and vaporization are fast in comparison to the laser pulse duration. The thermal and optical properties of the sample influence the amount of material removed during the laser pulse. The optical properties (absorption and reflection) determine both the fraction of the incident power that is absorbed and the depth of optical absorption within the sample. Different heating and cooling rates are expected if the depth of absorption is greater or less than the thermal diffusion length in the material. Although this interaction is defined as vaporization, the energy is delivered in a very short time and it is also localized. Thermodynamic models do not completely describe the interaction. Also, optical and thermal properties of the material vary during the laser pulse, which makes it difficult to accurately predict the amount of energy coupled to the target and the quantity of mass removed. The interaction is predominantly thermal. Melting is common and fractional vaporization is possible. That is, elements of higher vapor pressure will be enriched in the vapor relative to their concentration in the solid.

Ablation is another important component in pulsed laser deposition. At higher irradiance, beyond 1 Giga Watt per square centimeter with nanosecond and shorter laser pulses focused onto *any* material, an *explosion* occurs. The term "laser ablation" has been adopted to describe this interaction; it must sound better than "laser explosion". Phenomenologically, the surface temperature is *instantaneously* heated past its vaporization temperature through linear one-photon absorption, multi-photon absorption, dielectric breakdown, and additional undefined mechanisms. The vaporization temperature of the surface is exceeded within a fraction of the laser pulse duration; energy dissipation through vaporization from the surface is slow relative to the laser pulse width. Before the surface layer can vaporize, underlying material will reach its vaporization temperature. Temperature and pressure of the underlying material are raised beyond their critical values, causing the surface to explode. The pressure over the irradiated surface from the recoil of vaporized material can be extremely high. This explosive interaction has been described as "non-thermal", and melting is often not observed around the crater. During an ablative interaction, a plasma is initiated at the sample. Plasma temperatures are in excess of 10,000 K, and radiative heat transport can establish a *plasma-material interaction*. The plasma duration is microseconds, which is long in comparison to the short laser pulse. Power densities in the 1 Mega -1 Giga Watt per square centimeter range can cause vaporization, ablation, both of these processes simultaneously, or additional mechanisms that have not yet been identified. The continued interaction of the laser with the plasma provides high kinetic energies of the order of few tens to hundreds of eV to the ions and atoms of the plasma which is exploited for the low temperature growth under in-situ conditions. Hence, this technique is conceptually simple. A laser light enters through quartz window and is allowed to fall on the target kept inside the suitably evacuated deposition chamber after necessary focusing. As the laser source is kept outside the deposition chamber, virtually there is no constraint on varying deposition parameters such as in-situ pressure during growth as it is not going to affect the properties of electronic components.

Materials engineering requires stoichiometric thin films, high degree of reproducibility with least optimization steps. Furthermore, the relatively unexplored field of the fascinating science of nanomaterials requires a suitable method to produce them directly in nanostructured thin film form so as to get a quick first hand information about the physical properties of nanomaterials. As the engineering of the electronic structures can be done at atomic scales during layer by layer growth, a right thin film growth technique is necessary to explore. Pulsed laser deposition is very useful to quickly test the ideas about the materials with hybrid structures or meta-stable compounds which are otherwise difficult to form. The in-situ conditions such as oxygen partial pressure, substrate temperature and laser pulse energy provides the right opportunity to deposit nanostructured thin films of complicated meta-stable materials of relevance to technological applications. These conditions are very ideal to explore the gas sensing properties of chemical sensor material. Here we demonstrate the utility of this technique in deposition high quality sensor thin films for sensing gases at trace levels in the ambient.

Choice of the laser

Lasing wavelength:

Lasers that generate stoichiometric plume alone are useful and not all the lasers can be used for thin films growth. The stoichiometric ablation depends on the mechanism of interaction of the laser, which depends on the wavelength of the laser used. When laser light interacts with a solid surface, the amount of photon energy absorbed by the solid depends on the optical absorbance and thermo-physical properties of the solid. The increase in temperature leads to surface melting and evaporation, generating a plasma composed of neutral atoms, electrons and ions, in addition to particulates with dimensions ranging from nm to µm. Long wavelengths (> 500 nm), for example lasers like YAG lasers operating at fundamental 1064 nm or its first harmonic 532 nm have long optical penetration depth in the solid. Therefore, a large fraction of the laser pulse energy delivered to the surface of the solid will be used for thermal-like heating of a large volume leading to incongruent evaporation. The thermal-like heating component of the laser has to be minimized as for as possible for stoichiometric ablation. On the other hand, continuous lasers or lasers with long optical pulses with pulse durations of about few milliseconds provide the near equilibrium conditions for the thermal-like heating to set in which eventually leads to incongruent evaporation and non-stoichiometric plume. Besides, the ejection of larger particles (~µm size) directly from the solid target and the deposition of particulates over the films, it severely degrades the quality of the film. Moreover, at very high laser irradiance (above 50 J/cm^2), explosive boiling of the target material beneath the surface layer, as well as mass ejection of large particulates, may occur [**16**].

Shorter wavelength lasers with high pulse energies provide congruent evaporation and smoother thin films without unwanted particulates. Shorter the wavelength, smaller the penetration depth of the laser radiation into the material and hence ideally suitable for thin film deposition. For excimer lasers at 193 nm and 248 nm, the ablation depth is in the 100 nm range. For 157 nm, penetration depths are on the order of 50 nm. This short penetration depth results in very controlled layer-by-layer ablation with virtually no volume heating, thus eliminating the ejection of particulates. Additionally, the laser energy is deposited in a very restricted volume, and the quick and even material evaporation leads to clean ablation zones as shown in **Fig. 4**(a). The longer wavelength of Nd:YAG laser ablation induce melting and uncontrolled material splashing due to shallow energy density gradients as shown in **Fig. 4**(b).

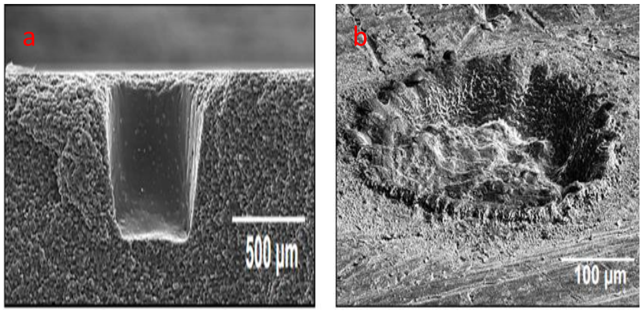

Fig. 4. (a) Shorter wave-length excimer laser yields clean ablation zones and (b) The longer wavelength of Nd:YAG laser ablation induces melting and uncontrolled material splashing.

Pulse energy:

High pulse energy is another important condition for pulsed laser thin film processing as it extends the range of target materials that can be ablated stoichiometrically. It also enables a larger area on the target to be ablated at a given fluence which subsequently increases the deposition rate and reduces the plume angle. It is generally observed that low pulse energy deposition leads to a gradual change in plume angle with time. This generally introduces inhomogeneity in thin films. Thus, the use of high pulse energy provides a high deposition efficiency and a larger process window, allowing consistent, successful deposition to be performed. Nd:YAG lasers can be operated at the fourth harmonic 266 nm after the necessary frequency conversion but the efficiency severely degrades toward shorter output wave-lengths. An overview of the optical performance parameters of excimer and flash-lamp pumped Nd:YAG lasers is given in the **Table I**. It is clear that excimer lasers have a high pulse energy at different UV wavelengths as compared to Nd:YAG lasers.

It is argued that the lasers with low pulse energy is sufficient for ablation as the rapidly expanding plasma plume of a high energy pulse shields the target from the beam, so that no significant ablation occurs after the first 5 ns of irradiation. This would imply that the pulse rise time is the most significant process parameter. However, this argument ignores the basic geometry of virtually of all PLD instrumentation wherein the laser hits the target at 30° to 50° angle. Thus, there is a minimum overlap with the plume which exits perpendicular to the target surface. Moreover, it has been established that the deposition rate increases with the increase in laser pulse energy [**17, 18**].

Table 1. Optical parameters of excimer and Nd:YAG lasers for thin film growth.

S.No.	Parameter	Excimer laser	Photon energy	Flash-lamp Nd:YAG laser
1.	Wavelength		*1.17 eV*	*1064 nm*
			2.33 eV	*532 nm*
		351 nm	3.53 eV	355 nm
		308 nm	4.02 eV	
			4.66 eV	266 nm
		248 nm	5.00 eV	
		193 nm	6.42 eV	
		157 nm	7.90 eV	
2.	Output energy	248 nm: 1200 mJ 193 nm: 600 mJ 157 nm: 50 mJ		355 nm: 200 mJ 266 nm: 100 mJ
3.	Repetition rate	1 – 200 Hz		10 Hz (fixed)
4.	Pulse to pulse stability	0.5 to 1 % rms		8 to 12 % rms
5.	Long term drift (4 hrs)	0 to 1 % rms		10 to 15 % rms
6.	Beam profile	Flat-top profile		"distorted Gaussian"
7.	Pulse width, FWHM	20 – 30 ns		5 to 8 ns

Pulse-to-pulse stability:

Uniform pulse energy is the single most critical laser output parameter for pulsed laser deposition (PLD) applications. For the film homogeneity, a constant pulse energy with least variations in pulse to pulse is required. Lasers with variable pulse energies not only brings in in-homogeneities in the film, but also non stoichiometry in the target compositions. **Table I** shows that excimer lasers have a good pulse to pulse stability as compared to Nd:YAG lasers.

Pulse width:

In order to rapidly reach the ablation threshold, the optimum laser pulse shape for PLD must have a fast rise time. This fast rise time must be followed by a pulse that is short enough to cause all material removal to occur by direct evaporation, rather than by melting. Lasers, with less than 3 ns rise time and pulse duration in the 20 ns range, are ideally suitable for PLD and both excimer and Nd:YAG lasers meet these criteria. **Table I** shows the pulse widths of excimer and Nd:YAG lasers.

Uniform beam profile:

A large, uniform beam profile with steep edges provides maximal use of the target, uniform ablation and smooth deposition. Excellent beam homogeneity over a well-defined flat-top spatial profile is ideally suitable which is provided by excimer lasers. **Fig. 5**(a) shows the beam profile of excimer laser with reasonable homogeneity [**19**]. Besides, the sharp falling of beam energy of excimer laser beam does not allow evaporation component to operate in that region. On the other hand, Nd:YAG lasers have inherently inappropriate Gaussian beam profile, relatively poor beam inhomogeneity leads and the gradual falling of beam fluence near the edges all of these factors lead to temperature-induced polarization and lateral distortions giving rise to nonstoichiometric plume. The typical beam profile of Nd: YAG laser is shown in **Fig. 5**(b). Hence, the criteria of laser for generating the stoichiometric plume are the short wavelength (UV), high pulse energy (a few hundreds of milli Joules), short pulse width (10 – 30 ns), high pulse to pulse stability (within 0.5%) and a well-defined flat-top spatial profile. In order to rapidly reach the ablation threshold, the optimum laser pulse shape for PLD must have a fast rise time. This fast rise time must be followed by a pulse that is short enough to cause all material removal to occur by direct evaporation, rather than by melting. Based on these reasons, a KrF excimer operating at a shorter wavelength (λ = 248 nm) and higher pulse energy is chosen for growing sensor grade thin films.

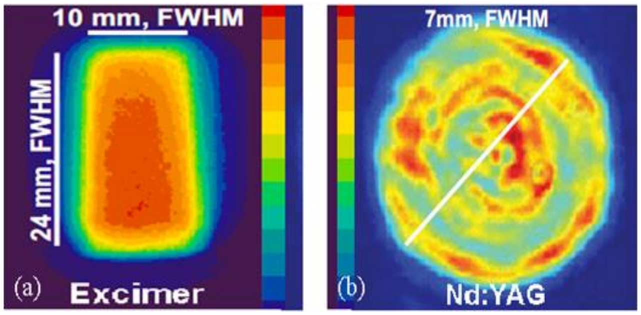

Fig. 5. (a) Excimer lasers with a well-defined flat-top homogeneous spatial profile and (b) Nd: YAG lasers with a in-homogeneous Gaussian profile

Experimental

One atom % Pd doped SnO_2, 0.5 at. % Ba doped In_2O_3, $Cr_{1.8}Ti_{0.2}O_3$ and $SrTi_{0.8}Fe_{0.2}O_3$ (identified based on preliminary screening experiments on gas sensing characteristics respectively for H_2, NO_x, NH_3 and % levels of O_2) were prepared by solid state method using stoichiometric amounts of SnO_2 and Pd, $BaCO_3$ and Cr_2O_3 and TiO_2, In_2O_3, $SrCO_3$, TiO_2 and Fe_2O_3 for the above compositions. The mixtures were heated at high temperatures and reground, compacted (1.5 cm diameter and 3 mm thickness) and again sintered at suitable temperatures. The process was repeated several times to achieve homogeneous samples. These pellets were used as targets for pulsed laser deposition of thin films on (100) $LaAlO_3$, (1102) Sapphire and polished alumina substrates. The parameters used during the deposition are given **Table II**. The thickness of all the films are generally about ~ 3000 Å. Crystallographic phase formation was checked by X-ray diffraction (Model D500, Siemens X-ray diffractometer, Germany) and the surface morphology was examined by atomic force microscopy (Solver Pro, NT-MDT, Russia). Prior to the deposition of thin film deposition, a meander type pattern of platinum heater was screen printed on the rear side of the substrate. Gold electrodes (1 mm × 2 mm) were also screen printed for making electrical contacts with the sensing film and with heater respectively. The substrate with screen printed heater patterns and gold electrical pads was mounted on a Teflon disc of 25 mm diameter and 3 mm thickness and the sensor assembly was enclosed in a SS or glass container of about known volume provided with sample injection port, air inlet and air outlet. Temperature of the sensing film can be controlled by passing known current through the heater and the gas sensing characteristics were studied temperatures between 200°C and 400°C at an interval of 50°C typically. At each temperature, the sensing film was equilibrated till a steady baseline resistance in air was observed. An appropriate amount of the analyte gas was then injected into the test chamber through the injection port, and the resistance was measured as a function of time till a steady final resistance was attained. The target gas was procured from commercial source was used for all testing purpose. The test chamber was then purged with air for about 2 min, and the sensor was allowed to reach its initial resistance value before the next experiment was carried out. The sensitivity for a given concentration of analyte gas was calculated as:

$$\text{Sensitivity} = R_g / R_a$$

where R_g = resistance of the film in air containing the analyte gas and R_a = resistance of the film in clean air. Each composition is tested for the cross-sensitivity to different concentrations of gases other than the intended gas.

Table II. Typical deposition conditions employed for depositing the sensor grade nanostructured thin films.

S.No.	Deposition parameters	Optimized values
1.	Laser wavelength	248 nm (KrF)
2.	Fluence	3 – 5 J/cm^2
3.	Repetition rate	7 - 10 Hz
4.	Preablation	3 min
5.	Ablation	20 min
6.	In-situ oxygen partial pressure	200 mtor
7.	Substrate- Target distance	4 cm
8.	Substrate temperature	400 – 550°C depending on the composition
9.	Substrates on which the thin films are grown	(100) $LaAlO_3$, (1102) Sapphire and polycrystalline Al_2O_3
10.	Compositions of the targets identified based on screening studies	1. Pd doped SnO_2 for ppm levels of H_2 2. 0.5 at. % Ba doped In_2O_3 for ppm levels of NO_x 3. $Cr_{1.8}Ti_{0.2}O_3$ for trace levels of NH_3 4. $SrTi_{0.8}Fe_{0.2}O_3$ for % level O_2

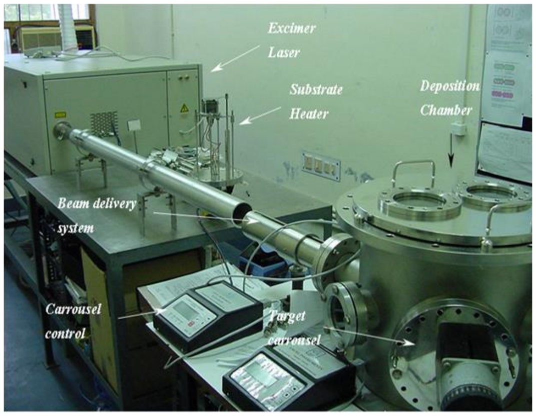

Fig. 6. Pulsed laser (KrF: λ = 248 nm, 20 Hz) deposition system with automated mutitarget control system and heater facility commissioned in our laboratory.

The typical deposition conditions employed for depositing the thin films of SnO_2, a well studied sensor material is given in **Table II**. **Fig. 6** shows the photograph of the PLD facility set up in the author's laboratory with multi-target carrousel assembly and the heater flange assembly.

Fig. 7 shows the general configuration adopted for all chemical sensors specific to different gases. The top side of the alumina substrate shows the sensing film is connected with gold pads for electrical leads as shown in **Fig. 7**(a) whereas the rear surface is coated with the thick film based inter-digited heater as shown in **Fig. 7**(b) [**20**].

Results and discussion

SnO_2 based H_2 sensors for applications in harsh environment

In the heat exchanger facility of the fast breeder reactors, any leakage from the pressurized steam into the secondary coolant sodium circuit will generate heat, NaOH in addition to hydrogen. During low power generation or start-up, this leak which propagates due to the presence of caustic alkali hydroxide has to be detected at the inception. Continuous monitoring of hydrogen evolved in the argon cover gas over sodium system provides the direct evidence of any such leakage [**20**]. The sensors which can monitor H_2 in argon cover gas have to be reliable, compact and rugged to operate in this harsh industrial environment.

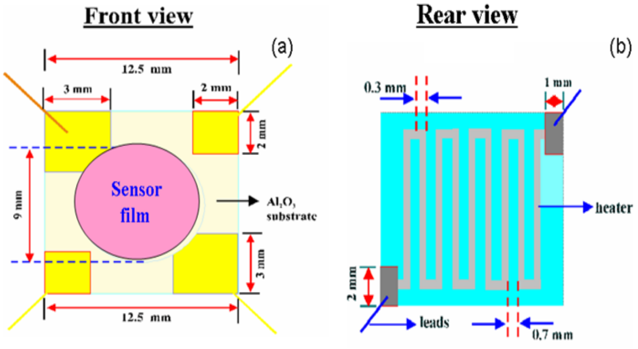

Fig. 7. General configuration adopted for all chemical sensors specific to different gases with gold pads (a) Sensing material on the top surface (b) Heater printed at the rear surface of the substrate.

A thermal conductivity detector (TCD) based diffusion type sensor was developed and is being used to monitor hydrogen levels in the argon cover gas. This sensor employs a hot nickel membrane in the form of a coiled tube through which hydrogen in cover gas of sodium circuit diffuses. This diffused hydrogen is swept away by an argon carrier gas and is analyzed by a thermal conductivity detector. Operating experience has shown that the lowest detection limit of this sensor is 30 ppm of hydrogen in argon. In order to extend the detection to still lower concentrations, surface conductivity based sensor with tin oxide is developed in our laboratory. Earlier, Pd-doped SnO_2 has been identified based on the screening studies to be promising sensing element for hydrogen. In this work, the use of PLD made tin oxide films of Pd-doped SnO_2 in a sensor device for this application is described.

Fig. 8 shows the XRD patterns of thin films of SnO_2 deposited on (100) $LaAlO_3$ and (1102) Sapphire substrates at different temperatures. Films were textured and the direction of orientation depends on the substrate as well as the growth temperature. Films grown at higher substrate temperatures were highly oriented and the degree of texturing decreases with decrease in growth temperature. To investigate the degree of orientation and the granular characteristics, TEM images of the films were recorded.

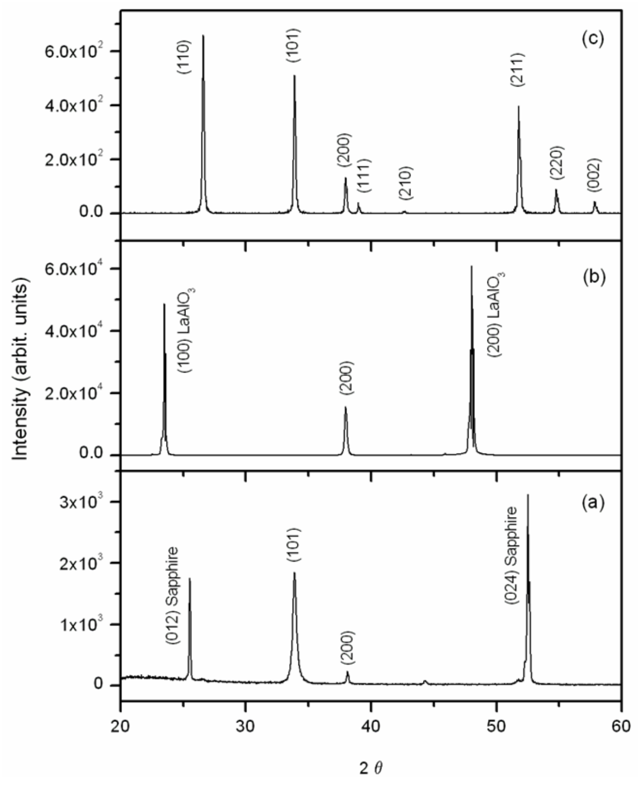

Fig. 8. XRD patterns of thin films of SnO_2 deposited at 500oC on (a) (1102) Sapphire (b) (100) $LaAlO_3$ substrates and (c) bulk SnO_2 target.

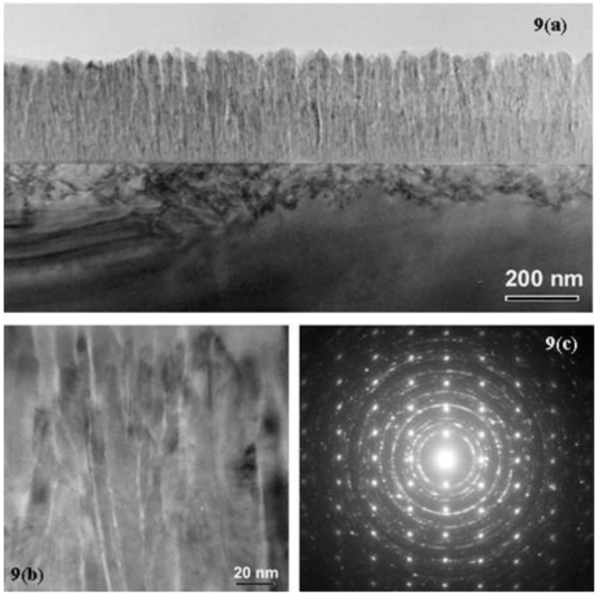

Fig. 9. TEM image of SnO_2 thin films deposited on (100) $LaAlO_3$ (a) Cross-sectional images (b) HRTEM image (c) SAED pattern.

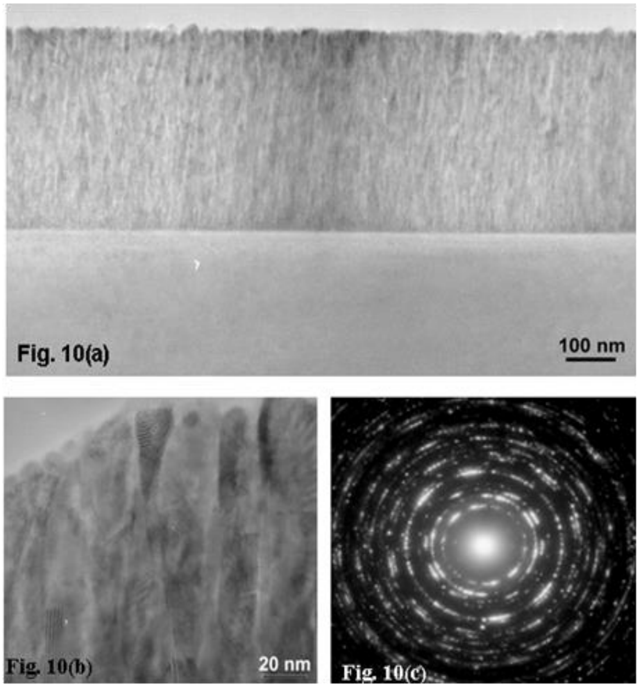

Fig. 10. TEM image of SnO_2 thin films deposited on (1102) Sapphire (a) Cross-sectional images (b) HRTEM image (c) SAED pattern.

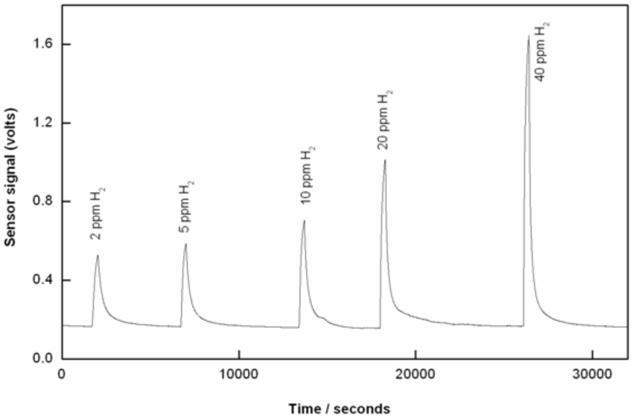

Fig. 12. The response pattern of pd doped SnO_2 thin film towards 1- 20 ppm of H_2 at 300°C.

Fig. 9(a) shows the cross-sectional HRTEM images of thin films of SnO_2 deposited on (100) $LaAlO_3$. It shows the film exhibits a granular morphology and is composed of 'long strands' starting from the substrate and extending up to the surface of the film with length matching the thickness of the film. The diameter of the strands varies from 6 to 14 nm depending on the growth temperature as revealed by the HRTEM image [**Fig. 9**(b)]. **Fig. 9**(c) shows the SAED pattern of these films, which show a powder pattern superimposed with the characteristic single crystalline nature. Films grown on (1102) sapphire also exhibits similar characteristics with a strand diameter slightly lower, typically around 6 to 10 nm as seen from **Fig. 10**(a & b). **Fig. 10**(c) shows the SAED pattern of these films, which conforms to the powder characteristics. To confirm the granular characteristics of the films, TEM image of the film after etching a portion of the substrate is recorded and shown in **Fig. 11**. Clearly, the films are highly granular and that the dimensions of the grain vary from 8 to 14 nm. It has been reported that the Debye length for SnO_2 is about 3 nm and therefore the necessary condition to get high sensitivity is that the grain size should be 2 × L_D which is about 6 nm [**10,11**]. Films grown under these conditions give an average grain size of about 8 to 14 nm. Films grown at higher temperatures of about 700°C tend to be highly textured and moving close to the epitaxial quality as the high temperature drives the coalescence of the smaller crystals and aligns them in the preferred direction. As anticipated, sensor grade quality of thin films deposited on polycrystalline Al_2O_3 under identical conditions will be highly sensitive to trace levels of H_2 and the response pattern of SnO_2 sensor for different concentrations of H_2 at 300°C is shown in **Fig. 12**. The film responds to 1 to 20 ppm of H_2 reproducibly and reliably [**20**].

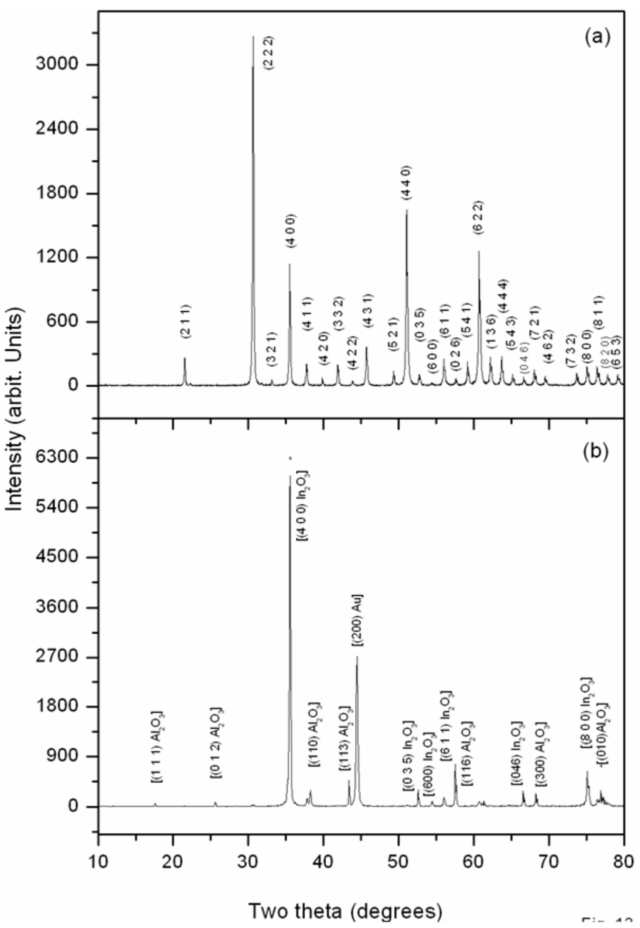

Fig. 13. XRD pattern of (a) Thin film of 0.5 at. % Ba doped In_2O_3 deposited at 500°C on polycrystalline alumina substrate (b) Bulk target.

Ba doped In_2O_3 sensor for sensing trace levels of NO_x in reprocessing industry

Automobiles, petrochemical industries, coal and natural gas power plants produce 100 – 2000 ppm of NO_x, a general name for the mixture of NO and NO_2 [**21**]. Both NO and NO_2 are highly toxic gases with threshold limit values (TLV – the highest permitted concentration for continuous inhalation for 8 hours without health risks) of 25 and 3 ppm respectively with pulmonary toxicity of NO_2 several times higher than that of NO. Besides, NO_x catalyses the formation of toxic ozone in the troposphere and participates in a chain reaction that destroys the protective stratospheric ozone layer. Hence, there is an urgency to develop highly reliable compact devices for continuous on-line monitoring of trace levels of NO_x in the ambient in order to prevent environmental disasters and extended health problems.

The XRD pattern of the thin film of 0.5 at. % Ba doped In_2O_3 deposited at 500°C on polycrystalline alumina substrate is shown in **Fig. 13**(b). Thin films were predominantly textured exhibiting (400) orientation. In addition, reflections corresponding to the XRD pattern of the substrates are also seen. For comparison, the XRD pattern of target is indexed in terms of the body centered cubic structure of In_2O_3 (space group: $I2_13$) [**Fig. 13**(a)].

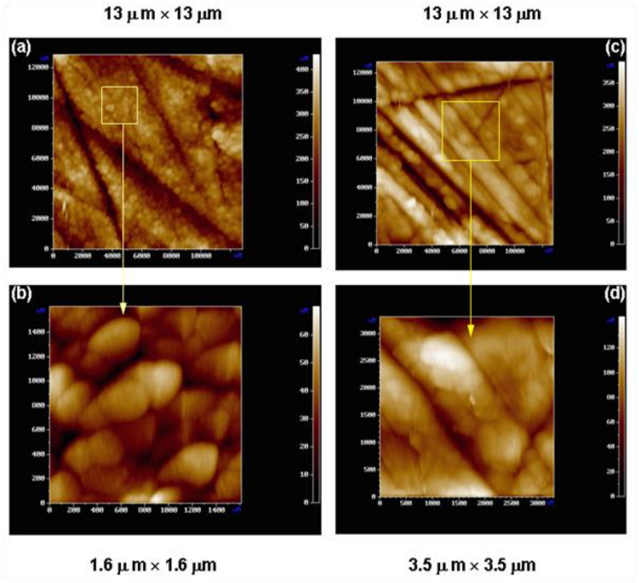

Fig. 14. AFM images recorded on (a) 13 μm × 13 μm scan area on thin film (b) 1.2 μm × 1.2 μm on thin film (c) 13 μm × 13 μm scan area on the bare substrate (b) 1.2 μm × 1.2 μm of the substrate

AFM images of textured thin films show a highly granular morphology as seen from **Fig. 14**(a) recorded on 13 μm × 13 μm scan area. The high resolution image scanned over an area of 1.6 μm × 1.6 μm shows that the average grain size is about 120 nm [**Fig. 14**(b)]. For comparison, the morphology of the bare substrate revealing granular characteristics containing long channels formed as a result of mechanical polishing [**Fig. 14**(c)]. The average grain size is about 5 μm as seen from the magnified image scanned over an area of 1.6 μm × 1.6 μm [**Fig. 14**(d)]. This granular morphological feature is the ideal configuration as it provides the required high specific surface area with a high probability of chemical interaction of the gaseous species.

Considering the sensitivity, response and retrace times, an operating temperature of 300°C is chosen and thin film sensors were tested for different concentrations of NO_x. The transient changes in resistance of the film on exposure to air containing 0.5, 1, 2, 5 and 10 ppm of NO_x at 300°C is recorded which shows that the sensitivity increases with the concentration of the NO_x as shown in **Fig. 15**. These experiments were repeated several times and results indicated the reproducibility of the gas sensing behaviour.

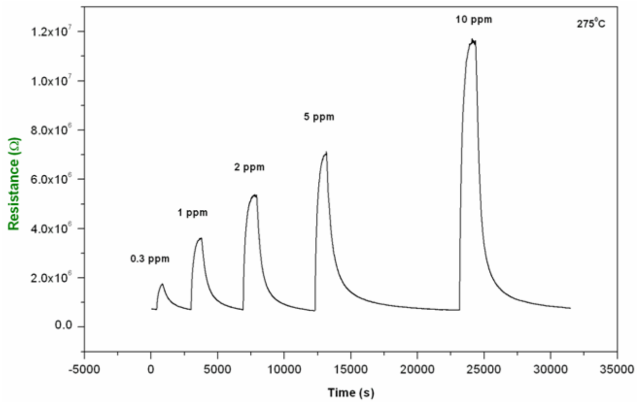

Fig. 15. The transient changes in resistance of the sensor on exposure to air containing 0.5, 1, 2, 5 and 10 ppm of NO_x at 300°C.

$CrTiO_3$ based thin film sensor for sensing trace levels of NH_3

Sensors for monitoring trace levels of ammonia are needed for the safety of the working personnel and the environment safety especially in chemical, fertilizer and petrochemical industries handling large quantities of ammonia. Heavy water enrichment industries which use NH_3 need rugged, compact and reliable ammonia sensing devices that can respond to trace levels of ammonia in air typically 1 - 25 ppm as the TLV limit is about 25 ppm [**22**]. Based on the screening studies $Cr_{1.8}Ti_{0.2}O_3$ is identified as the promising candidate for sensing ammonia. Nanostructured thin films of $Cr_{1.8}Ti_{0.2}O_3$ were deposited by PLD and the results are described.

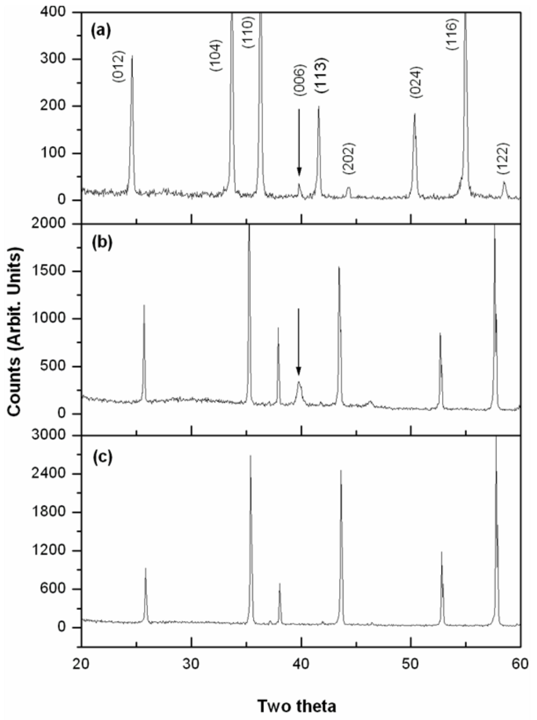

Fig. 16. XRD patterns of (a) Bulk $Cr_{1.8}Ti_{0.2}O_3$ (b) Thin films of $Cr_{1.8}Ti_{0.2}O_3$ deposited on polycrystalline Al_2O_3 substrates (c) Bare polycrystalline Al_2O_3 substrate.

The XRD patterns of thin films of $Cr_{1.8}Ti_{0.2}O_3$ deposited on polycrystalline Al_2O_3 substrates shows that they were highly (00l) oriented due to a strong line corresponding to the (006) reflection [**Fig. 16**]. For comparison, the XRD patterns of bare Al_2O_3 substrate and that of bulk $Cr_{1.8}Ti_{0.2}O_3$ were also shown. No other line corresponding to any impurity phase is detected implying that the film grown as a single pure phase. It must be noticed that the formation of $Cr_{1.8}Ti_{0.2}O_3$ phase in bulk starts only above 900°C and below 500°C there is no formation of the phase. However, the phase is stabilized at 500°C in thin film form which might be due to the extra energy given by the laser photons to each of the ions/molecules or atoms.

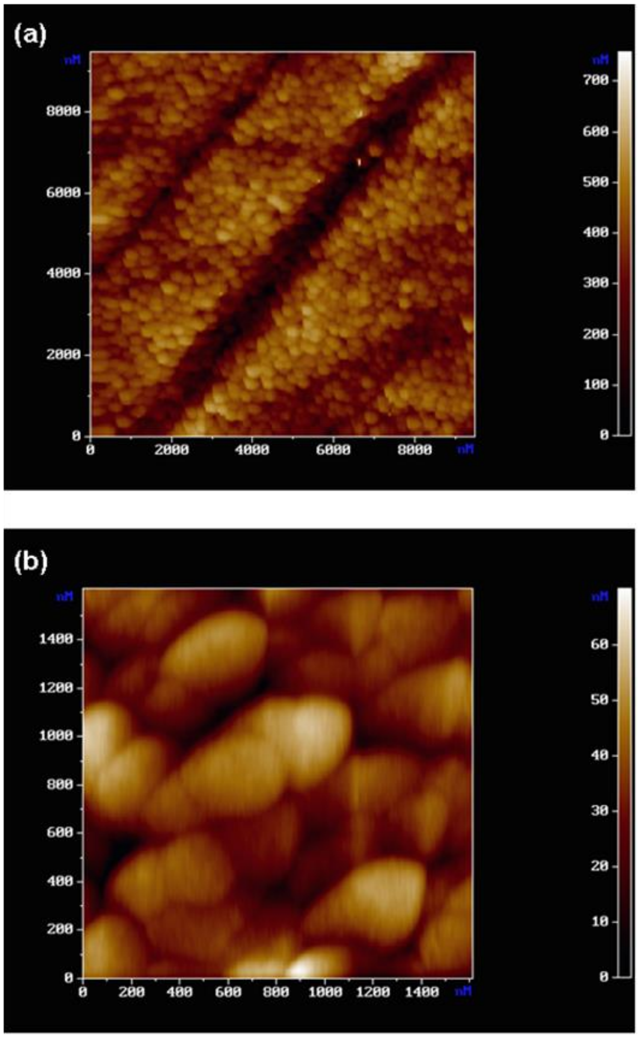

Fig. 17. AFM images of the thin films of $Cr_{1.8}Ti_{0.2}O_3$ grown on polycrystalline Al_2O_3 substrates at 500°C (a) 10 µm × 10 µm scan area (b) 1.2 µm × 1.2 µm scan area.

AFM images of the thin films of $Cr_{1.8}Ti_{0.2}O_3$ grown on polycrystalline Al_2O_3 substrates at 500°C exhibit a highly granular, composed of grains of nearly uniform size [**Fig. 17**(a)] The effect of mechanical polishing of the polycrystalline substrate is reflected in terms of scratches as seen from the **Fig.** A high resolution image of film shows that the average grain size is about 100 nm [**Fig. 17**(b)]. **Fig. 18** shows the response characteristics of $Cr_{1.8}Ti_{0.2}O_3$

grown on polycrystalline Al_2O_3 substrates at 500°C. Films respond to trace levels of ammonia in air typically ranging from 1 ppm to 20 ppm. The threshold limit value of ammonia is about 25 ppm.

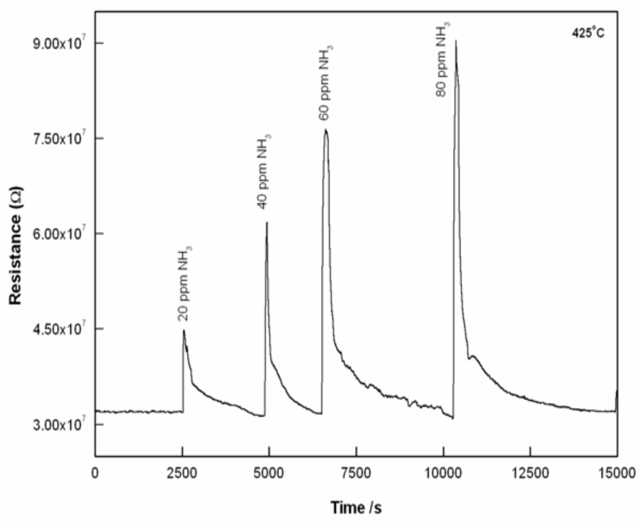

Fig. 18. Typical response pattern thin films of $Cr_{1.8}Ti_{0.2}O_3$ at 400°C towards ammonia grown on polycrystalline Al_2O_3 substrates at 500°C.

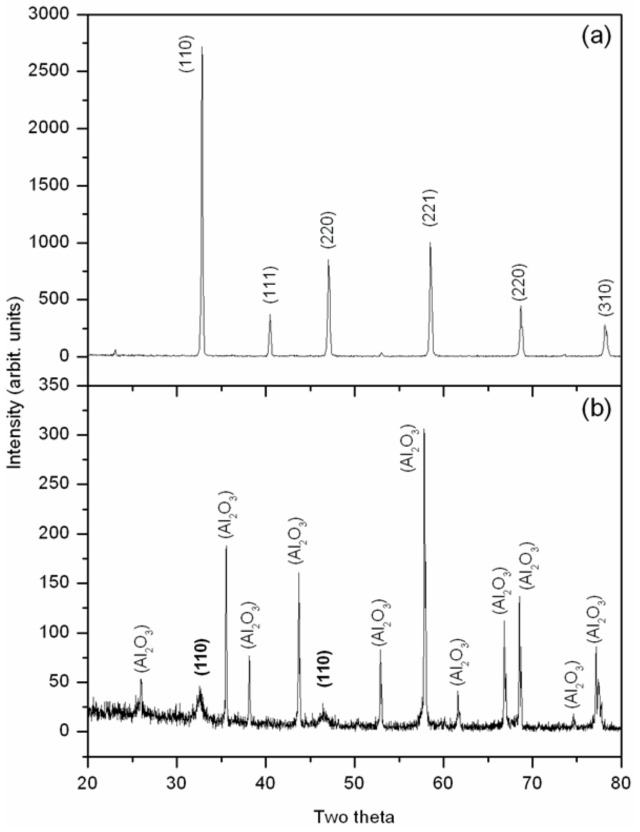

Fig. 19. The XRD patterns of (a) Bulk $SrTi_{0.8}Fe_{0.2}O_3$ target (b) Thin films of $SrTi_{0.8}Fe_{0.2}O_3$ deposited on polycrystalline Al_2O_3 substrates

$SrTi_{1-x}Fe_xO_3$ (0.1 < x < 0.4) thin films for percentage level oxygen sensing

Sensors for monitoring percentage level changes in oxygen are required to ensure the safety of the working personnel in and around the closed industrial environment handling large volumes of inert gases as any accidental release would bring down the oxygen partial pressure drastically causing asphyxiation. Breeder reactors use large quantities of argon as cover gas and therefore, the oxygen partial pressure in the reactor operating area has to be continuously monitored [**23**]. Therefore, highly sensitive, rugged, compact and reliable oxygen sensing devices which can respond to changes in percentage levels of oxygen from 10 to 20 % are required. Based on the screening studies $SrTi_{0.8}Fe_{0.2}O_3$ is identified as the promising candidate for sensing ammonia. Nanostructured thin films of $SrTi_{0.8}Fe_{0.2}O_3$ were deposited by PLD and the results are described.

The XRD patterns of thin films of $SrTi_{0.8}Fe_{0.2}O_3$ deposited on polycrystalline Al_2O_3 substrates shows that they were highly (00l) oriented due to the presence of a strong (006) reflection [**Fig. 19**]. For comparison, the XRD patterns of bare Al_2O_3 substrate and that of bulk $SrTi_{0.8}Fe_{0.2}O_3$ were also shown. No other line corresponding to any impurity phase is detected implying that the film grown as single phase. It must be noticed that the formation of $SrTi_{0.8}Fe_{0.2}O_3$ phase in bulk starts only above 900°C and below 500°C there is no formation of the phase. However, the phase is stabilized at 500°C in thin film form which might be due to the extra energy given by the laser photons to each of the ions/molecules or atoms. **Fig. 20** shows the response characteristics of $SrTi_{0.8}Fe_{0.2}O_3$ grown on polycrystalline Al_2O_3 substrates at 425°C for different partial pressures of oxygen. Films respond quite reliably and reproducibly when the oxygen partial pressure is varied for 5 to 20 %. The response and retrace times are typically 5 and 30 seconds respectively.

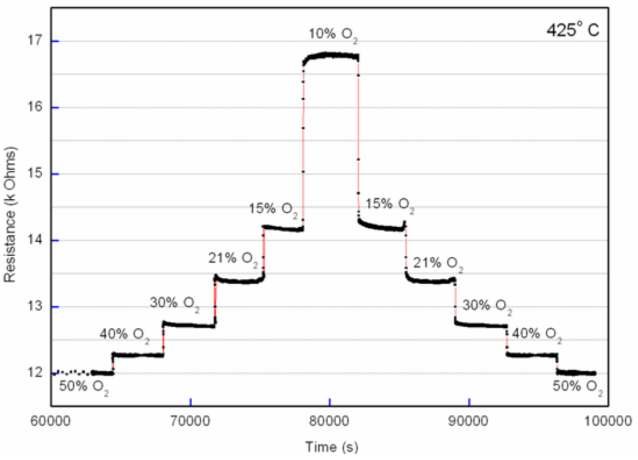

Fig. 20. Response pattern of $SrTi_{0.8}Fe_{0.2}O_3$ grown on polycrystalline Al_2O_3 substrates at 500°C for different partial pressures of oxygen.

Conclusion

High quality sensor grade nanostructured thin films of multicomponent oxide material can be deposited by pulsed laser deposition technique without tedious optimization procedures. Materials which are not amenable to synthesis using solution chemical methods as nanocrystals can conveniently be deposited as nanostructured thin films by this technique and thus it offers the scope of pursuing the science of nanomaterials in thin film form. Nanostructured thin films of selected materials each specific to a particular gaseous species at trace levels ppm levels are deposited and their response to different gases is demonstrated.

Acknowledgements

The authors are thankful to Dr. K.V.G. Kutty and Mr. Asuvathraman for their help in XRD.

Reference

1. Handbook of Thin Film Process Technology, Editors: Glocker, D. A.; Shah, S. I. (Eds.); Institute of Physics Publishing: Philadelphia, USA, 1998.
2. Chrisey, D. B.; Inam, A. MRS Bull. 1992, 17, 37.
3. Cheung, J. P; Sankur, J.; CRC Critical Reviews, Sol. State Mater. Sci. 15, 63 (1988).
   DOI: 10.1080/10408438808244625.
4. Geraint Williams and Gary S.V. Coles, MRS Bull. 1999, 24, 25.
5. Zhang,S.; Sun, D.; Fu Y.; Du, H.; Surf. Coat. Technol. 2003, 167, 113.
   DOI: 10.1016/S0257-8972(02)00903-9.
6. Gopel, W.; Schierbaum, K.D. Sens. Actuators. 1995, B 26, 1.
   DOI: 10.10160925-4005(94)01546-T.
7. Yamazoe, N.; Miura, N. In Chemical Sensor Technology; Yamamuch (Eds.); Japan, **1992**, Vol - 4, pp. 20 - 30.
8. Williams, D. E. In Solid state gas sensors; Mosley, P.T.; Tofield, B.C. (Eds.); Adam Hilger, USA, **1987**, pp. 71 - 89.
9. Moseley P.T.; Tofield, B.C. In Solid State Gas Sensors; Moseley P.T.; Tofield, B.C. (Eds.); Adam Hilger, Phiadelphia, USA, 1987.
10. Mitzei, J. Sensor and Actuators. 1995, B 23, 173.
    DOI: 10.1016/0925-4005(94)01269-N.
11. Shimizu, Y; Egashira, M. MRS Bull. 1999, 24, 18.
12. Hubler, G.K. MRS Bull. 1992, 17, 26.
13. Smith, H. M.; A. F. Turner, Appl. Opt. 1965, 4,147.
14. Venkatesan, T.; Wu, X.D.; Inam, A.; Watchman, J. B. Appl. Phys. Lett. 1988, 52, 1193.
    DOI: 10.1063/1.99672.
15. Cheung, J; Horwitz, J. MRS Bull. 1992, 17, 30.
16. Foltyn, S. R.; Dye, R. C.; Ott, K. C.; Hubbard, K. M.; Hutchinson, W.; Muenchausen, R. E.; Estler, R. C.; Wu, X. D. Appl. Phys. Lett. 1991, 59, 594.
    DOI: 10.1063/1.105386.
17. Delmdahl, R.; Paetzel, R. Appl. Phys. 2008, A 93, 611.
    DOI: 10.1007/S00339-008-4716-7.
18. Delmdahl R.; Pätzel, R. Phys. Stat. Sol. 2008, C 5, 3276.
    DOI: 10.1002/pssc.200779515.
19. Basting, D.; Pippert, K.; Stamm, U, RIKEN Review 2002, 43, 14.
20. Prabhu, E.; Jayaraman, V.; Gnanasekar, K.I.; Gnanasekaran, T.; Periaswami, G. Asian J. Phys. 2005, 14, 33.
21. Shekhar, C.; Gnanasekar, K.I.; Prabhu, E.; Jayaraman, V.; Gnanasekaran, T. Sensors and Actuators 2011, B 155, 19.
    DOI: 10.1016/J.snb.2010.08.025.
22. Jayaraman, V.; Gnanasekar, K.I.; Prabhu, E.; Gnanasekaran T.; Periaswami, G. Sensors and Actuators 1999, B 55, 175.
    DOI: 10.1016/S0925-400(99)00052-O.
23. Misra, S.; Prabhu, E.; Gnanasekar, K. I.; Jayaraman, V.; Chandramohan, P.; Srinivasan M. P.; Gnanasekaran, T., Proceedings of the Intl. Conference on Sensors and Related Networks; Raina, J.P.; Alex, Z.C.; Satyamurthy, S. A. V.; Sudhir, S.K.; Arulmozhivarman, P. (Eds.); Allied Publishers Pvt. Ltd, India, 2007, pp. 66.